

Multi-wavelength optical determination of black and brown carbon in atmospheric aerosols

D. Massabò ^{a,*}, L. Caponi ^a, V. Bernardoni ^b, M.C. Bove ^a, P. Brotto ^a, G. Calzolari ^c,
F. Cassola ^a, M. Chiari ^d, M.E. Fedi ^d, P. Fermo ^e, M. Giannoni ^d, F. Lucarelli ^{c,d}, S. Nava ^d,
A. Piazzalunga ^f, G. Valli ^b, R. Vecchi ^b, P. Prati ^a

^a Dept. of Physics, University of Genoa & INFN, Via Dodecaneso 33, 16146, Genova, Italy

^b Dept. of Physics, Università degli Studi di Milano & INFN, Via Celoria 16, 20133, Milano, Italy

^c Dept. of Physics, University of Florence, Via Sansone 1, 50019, Sesto Fiorentino, FI, Italy

^d INFN – Section of Florence, Via Sansone 1, 50019, Sesto Fiorentino, FI, Italy

^e Dept. of Chemistry, Università degli Studi di Milano, Via Golgi 19, 20133, Milano, Italy

^f Dept. of Environmental and Territorial Sciences, Università degli Studi di Milano-Bicocca, Piazza della Scienza 1, 20122 Milan, Italy

A B S T R A C T

In this paper, a new way to apportion the absorption coefficient (b_{abs}) of carbonaceous atmospheric aerosols starting from a multi-wavelength optical analysis is shown. This methodology can disentangle and quantify the contribution to total absorption of equivalent black carbon (EBC) emitted by wood burning (EBC_{WB}) and fossil fuel (EBC_{FF}) as well as brown carbon (BrC) due to incomplete combustion. The method uses the information gathered at five different wavelengths in a renewed and upgraded version of the approach usually referred to as Aethalometer model. Moreover, we present the results of an apportionment study of carbonaceous aerosol sources performed in a rural area and in a coastal city, both located in the North-West of Italy. Results obtained by the proposed approach are validated against independent measurements of levoglucosan and radiocarbon. At the rural site the EBC_{WB} and EBC_{FF} relative contributions are about 40% and 60% in winter and 15% and 85% in summer, respectively. At the coastal urban site, EBC_{WB} and EBC_{FF} are about 15% and 85% during fall. The OC contribution to the wood

* Corresponding author.

E-mail address: massabo@ge.infn.it (D. Massabò).

burning source at the rural site results approximately 50% in winter and 10% in summer and about 15% at the coastal urban site in fall. The new methodology also provides a direct measurement of the absorption Ångström exponent of BrC (α_{BrC}) which resulted $\alpha_{\text{BrC}} = 3.95 \pm 0.20$.

1. Introduction

Carbonaceous aerosols play an important role in environmental issues like air quality, human health and global climate change. Although the classification of carbonaceous aerosol components is still under debate (Pöschl, 2003), total carbon (TC) is generally divided in black carbon (BC), organic carbon (OC) and carbonate carbon (CC).

Amongst atmospheric aerosols, BC is considered the most efficient light-absorber in the visible spectrum (Bond et al., 2013; and reference therein) with a weak dependence on wavelength (λ) (Moosmüller et al., 2009). Another light-absorbing component of carbonaceous aerosols is the so-called brown carbon (BrC) (Andreae and Gelencsér, 2006; Pöschl, 2003), the fraction of organic carbon with increased absorbance in the blue and ultraviolet (UV) region of the solar spectrum (Moosmüller et al., 2011). Carbonaceous light-absorbing particles are typically emitted by incomplete combustion of fossil fuels related to traffic, industrial processes and domestic heating as well as by biomass burning.

It is worthy to note that beyond carbonaceous aerosols, also other aerosol components show strong light-absorbing properties like iron oxides in mineral dust particles (Linke et al., 2006).

The spectral dependence of the aerosol absorption coefficient (b_{abs}) is generally described by the power-law relationship $b_{\text{abs}}(\lambda) \propto \lambda^{-\text{AAE}}$ where the AAE is the Ångström absorption exponent (Moosmüller et al., 2011). In literature works AAE has been shown to be sensitive to aerosol chemical composition but also to particle size and morphology (e.g. Kirchstetter et al., 2004; Lewis et al., 2008; Utry et al., 2014). In a large number of cases, it has been exploited as a chemically selective parameter useful to identify the aerosol origin and apportionment sources for different carbonaceous aerosols (Sandradewi et al., 2008; Ajtai et al., 2010; Favez et al., 2010; Flowers et al., 2010; Filep et al., 2013; Utry et al., 2013); nevertheless, Utry et al. (2014) claim that the assessment of aerosol microphysical properties is needed to retrieve more accurate results on the aerosol absorption properties. AAE values around 1 have been reported for BC and up to 9.5 for BrC (Lack and Langridge, 2013).

An advantage of the AAE determination in aerosol samples by multi- λ techniques is the possibility of performing on-line source apportionment studies as done by many authors in recent years to evaluate woodsmoke and traffic contributions adopting the so-called Aethalometer model (Sandradewi et al., 2008; Favez et al., 2010) thus avoiding time consuming laboratory analyses.

At the state of the art the measurement of light absorption is still challenging (Andreae, 2001; Moosmüller et al., 2011), notwithstanding filter-based on-line techniques (e.g. the Aethalometer; the Particle Soot Absorption Photometer; the Multi Angle Absorption Photometer, among others) are widespread but – with the exception of the Aethalometer – multi- λ analysis is generally not

implemented. There are some important drawbacks to be addressed in order to get reliable values from these filter-based instruments as it is well known that they are affected by measurement and sampling artifacts (e.g. effects due to multiple scatterings, to particle shadowing due to filter loading, absorption of organics; Bond et al., 1999; Collaud Coen et al., 2010; Vecchi et al., 2014; among others). Although not very widespread yet, photoacoustic spectroscopy operated at multi- λ (Lewis et al., 2008; Ajtai et al., 2010; Flowers et al., 2010) is currently the only method capable to overcome the above mentioned drawbacks in absorption measurements.

At the University of Genoa a Multi-Wavelength Absorbance Analyzer (MWAA) has been recently developed (Massabò et al., 2013) basing on the single- λ Multi Angle Absorption Photometer concept (MAAP, Petzold and Schöllinger, 2004; Petzold et al., 2005). Such instrumentation measures both transmitted and scattered light in the forward and back hemispheres thus reducing the cross-sensitivity to aerosol scattering components and filter loading effects (Müller et al., 2011). This approach does not need a posteriori data corrections necessary when attenuation measurements only are performed (e.g. Collaud Coen et al., 2010): such corrections are typically composition dependent and prevent real-time accurate source apportionment.

In this work, we present a new apportionment methodology together with an original data reduction approach developed using an up-graded version of the MWAA serving reliable b_{abs} data at different wavelengths. From the direct apportionment of BC and BrC spectral absorption properties, the contributions of fossil fuels (FF) and wood burning (WB) to the carbonaceous aerosols concentration can be disentangled.

2. The Multi-Wavelength Absorbance Analyzer (MWAA)

2.1. Set-up

A detailed description of the original MWAA set-up is given in Massabò et al. (2013) and in the following only major changes and upgrades will be reported.

The MWAA is basically composed by light emitting sources, an automatized sample-changer, and 4 low-noise UV-enhanced photodiodes. In the original configuration three low-power laser diodes ($\lambda = 407, 635, 850$ nm) were displaced on a slide and manually aligned thanks to mechanical benchmarks. In the new configuration, two laser diodes with $\lambda = 375$ nm and 532 nm (World Star Tech) have been added. A motorized stage has been added to interchange the laser sources thus improving the system stability and reproducibility and facilitating the analysis of many samples.

The 5- λ b_{abs} measurements are exploited in the model proposed in this paper to retrieve more accurate results (see §3). In particular, measurement at UV wavelength is useful because the absorption properties of atmospheric aerosols at this λ are generally poorly known and brown carbon is expected to strongly absorb in this

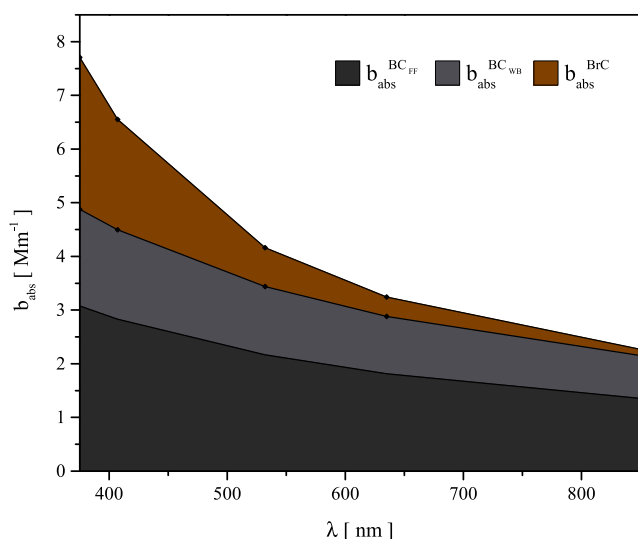


Fig. 1. Mean BC_{FF} , BC_{WB} and BrC light absorption coefficients as a function of wavelength at Propata during winter 2014.

range (Andreae and Gelencsér, 2006; Kirchstetter and Thatcher, 2012).

In the final configuration, the MWAA can perform 5-wavelength analysis of 16 filters/samples per session in less than 90 min measuring each filter in 64 different points, each $\sim 1 \text{ mm}^2$ wide.

2.2. Calculation of the aerosol absorption coefficient

To derive the b_{abs} at each measured λ , the MWAA partially follows the approach reported by Petzold and Schöllner (2004) and implemented in the MAAP. From the measurement of the light transmitted and scattered at fixed angles, the light angular distributions in the forward and in the back hemispheres are retrieved using analytical functions. Once the light distribution is obtained in both hemispheres (for details on the MWAA see Massabò et al., 2013), a radiative transfer model taking into account the multiple scattering effects occurring within the particle-filter system is applied (Hänel, 1987, 1994). The model gives the two parameters needed to calculate the sample absorbance (ABS – the fraction of light absorbed by the loaded filter), i.e. the total optical thickness (τ) and the aerosol-filter layer single scattering albedo (SSA). These parameters are linked to ABS through the relationship $ABS = \tau(1 - SSA)$. Finally, b_{abs} is given by $b_{abs} = ABS \cdot A/V$, where A is the active surface filter area and V is the volume of sampled air.

3. Field campaigns and laboratory analyses

3.1. Samples collection

PM10 aerosol samples were collected at two different locations in Liguria (Italy): a regional background and an urban background site. The regional background monitoring site was placed in a small village (Propata, $44^\circ 33' 52.93''N$, $9^\circ 11' 05.57''E$, 970 m a.s.l., population 160 inhabitants) in the Ligurian Apennines where wood burning is expected to be a major aerosol source especially during wintertime as it is used for both domestic heating and cooking. Due to its peculiar position, Propata can be occasionally impacted by pollution advection from the Po valley as well as from the coastal area at South. The urban background monitoring site was 2 km far from the Genoa city centre ($44^\circ 24' 08.93''N$,

$8^\circ 58' 18.17''E$, 60 m a.s.l., population 600,000 inhabitants). The sampling site was located on the terrace of the Physics Department and it can be considered as representative of a maritime urban background station because not directly influenced by local pollution sources.

In Propata the sampling covered different periods: February–July 2013 and November 2013–January 2014. 48-hour PM10 samples (120 in total) were collected on quartz-fibre filters (Pall, 2500QAO-UP, 47 mm diameter) using a low-volume sampler (38.3 l min^{-1} by TCR Tecora, Italy). Additional PM10 samples were collected for radiocarbon analysis on quartz-fibre filters (Pall, QAT-UP, 150 mm diameter) using a high-volume sampler (500 l min^{-1}). This sampling was carried out in March–April 2013. Each sampling lasted about 6 days and 4 samples were collected overall.

In Genoa 24-h PM10 was sampled for two weeks (October 31–November 13 2013) by a low-volume sampler (38.3 l min^{-1} by TCR Tecora, Italy). Aerosol particles were collected on quartz-fibre filters (Pall, 2500QAO-UP, 47 mm diameter).

The quartz-fibre filters were never heat-treated before sampling; any possible contamination was assessed in each batch before sampling (the maximum OC contamination was $1.7 \pm 0.3 \mu\text{g cm}^{-2}$). Field blank filters were used to monitor any possible further contaminations. Moreover, in this work we decided to neglect the possible effect of sampling artefacts due to organics on light absorption measurements when using quartz-fibre filters as shown by Vecchi et al. (2014) because it has been considered here not to alter the approach described in §3.

3.2. Laboratory analyses

Filters were weighed before and after the sampling in an air-conditioned room. After weighing, low-volume samples were analyzed by MWAA to retrieve b_{abs} at five different wavelengths. EC and OC were determined on one punch (1.5 cm^2) of the quartz-fibre filter by a Thermal Optical Transmittance (TOT) instrument (Sunset Lab Inc.) using the EUSAAR_2 protocol (Cavalli et al., 2010). In addition, levoglucosan – a well known marker for wood burning (Simoneit et al., 1999) – was determined by High Performance Anion Exchange Chromatography coupled with Pulsed Amperometric Detection on a portion of the same quartz-fibre filter (Piazzalunga et al., 2010).

TC radiocarbon analyses on high-volume samples were performed at the Accelerator Mass Spectrometry (AMS) facility of the INFN-LABEC laboratory of Florence (Italy) (see Fedi et al., 2013 for details). Sample preparation for AMS analysis was carried out using a sample preparation line suitably set up for aerosol samples (Calzolari et al., 2011), following the TC sample preparation procedure described in Bernardoni et al. (2013).

The measured $^{14}\text{C}/^{12}\text{C}$ was corrected for the background signal and then for isotopic fractionation according to $^{13}\text{C}/^{12}\text{C}$ measured in the accelerator. Data were normalized to the isotopic ratio obtained for the oxalic acid II standard NIST 4990C and the results were expressed as fraction of modern carbon (f_m) in the sample. It is noteworthy that nuclear weapon tests in the 50's and 60's led to the increase of ^{14}C – ^{12}C ratio in biogenic material. Thus, f_m must be corrected for reference values of the ^{14}C content for the sampling period ($f_{m,mod}$) to correctly apportion modern sources. In this work, $f_{m,mod}$ was set to 1.08, assuming equivalent contributions by wood combustion and biogenic sources and using 1.116 and 1.036 as representative f_m values for the wood burnt and the biogenic material, respectively (Zotter et al., 2014). The relative contribution from modern (non-fossil) sources was estimated as $f_{NF} = f_m/f_{m,mod}$.

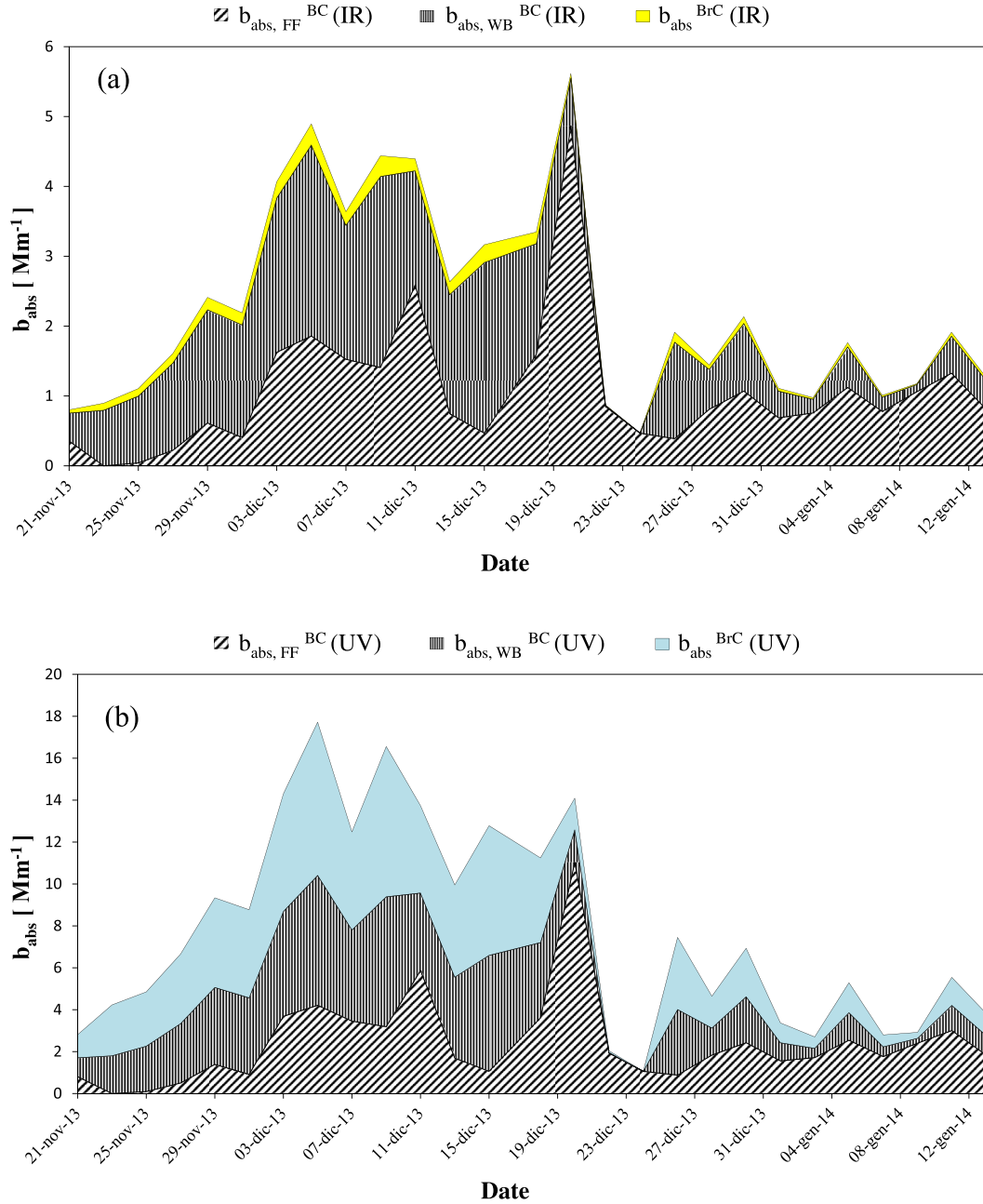


Fig. 2. Optical apportionment obtained at the rural site during wintertime 2014: (a) $\lambda = 850$ nm (IR) and (b) $\lambda = 375$ nm (UV).

4. Multi-wavelength analysis

4.1. Optical apportionment

In this work, a new source apportionment model (MWA approach) based on the measurement of b_{abs} at five wavelengths was developed. The MWA approach exploits the information provided by the 5- λ measurements to obtain directly the BrC AAE (α_{BrC}) and the BrC absorption coefficient ($b_{\text{abs}}^{\text{BrC}}$) at each measured λ . These are innovative features compared to the Aethalometer model (Sandradewi et al., 2008; Favez et al., 2010) which uses measurements at two λ only (even with the 7- λ instrument) and provides the total contribution to b_{abs} due to fossil fuels ($b_{\text{abs,FF}}$) and wood burning ($b_{\text{abs,WB}}$) without information on the species (i.e. BC or BrC)

responsible for such contributions.

The minimization algorithm used in the MWA approach joined to TOT measurements allows also to apportion the contributions of FF and WB to the EC (EC_{FF} and EC_{WB} , respectively) and, although with some further assumptions, to the OC (OC_{FF} and OC_{WB} , respectively).

The MWA approach starts from two different decompositions of $b_{\text{abs}}(\lambda)$.

In the first case, $b_{\text{abs}}(\lambda)$ is assumed to be the sum of the absorption coefficients of BC ($b_{\text{abs}}^{\text{BC}}(\lambda)$, regardless of its FF or WB origin), and BrC ($b_{\text{abs}}^{\text{BrC}}(\lambda)$), as follows

$$b_{\text{abs}}(\lambda) = b_{\text{abs}}^{\text{BC}}(\lambda) + b_{\text{abs}}^{\text{BrC}}(\lambda) \quad (1)$$

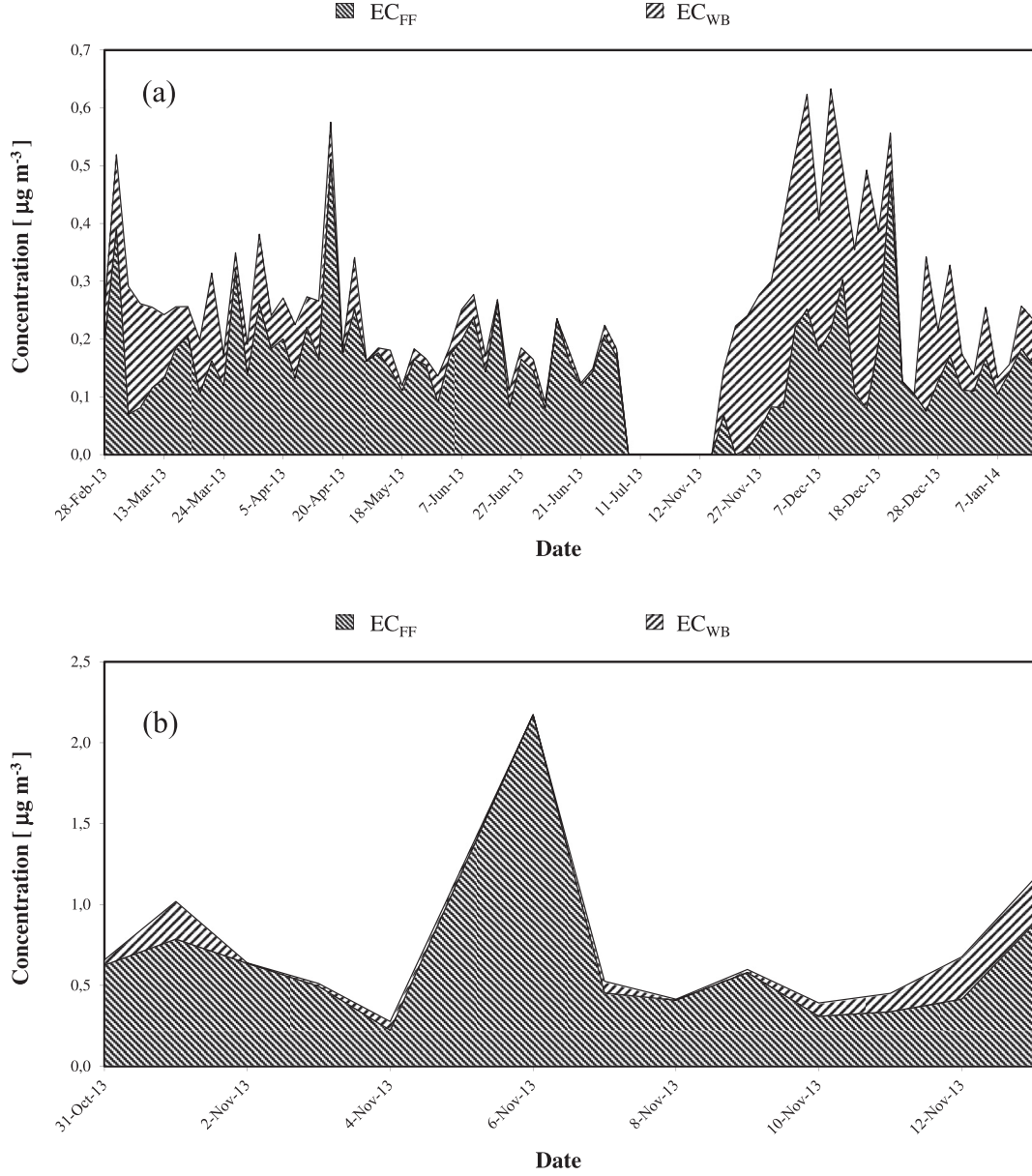


Fig. 3. EC apportionment at the rural site (a) and the urban background site (b).

Furthermore, $b_{abs}^{BC}(\lambda)$ and $b_{abs}^{BrC}(\lambda)$ are assumed to be λ -dependent following the general relationship $b_{abs}(\lambda) \propto \lambda^{-\alpha}$, where α is different for BC and BrC (α_{BC} and α_{BrC} , respectively). Thus, Eq. (1) can be written as:

$$\frac{b_{abs}^{BC}(\lambda_1)}{b_{abs}^{BC}(\lambda_{ref})} = \left(\frac{\lambda_1}{\lambda_{ref}}\right)^{-\alpha_{BC}} \quad \frac{b_{abs}^{BrC}(\lambda_1)}{b_{abs}^{BrC}(\lambda_{ref})} = \left(\frac{\lambda_1}{\lambda_{ref}}\right)^{-\alpha_{BrC}} \quad (2)$$

where λ_{ref} can be arbitrarily chosen.

In the second case, the decomposition approach is the same as in the Aethalometer model:

$$b_{abs}(\lambda) = b_{abs,FF}(\lambda) + b_{abs,WB}(\lambda) \quad (3)$$

where $b_{abs,FF}$ and $b_{abs,WB}$ are the contributions from FF and WB to the total b_{abs} . This decomposition assumes that FF and WB are the only sources of light absorbing species at the sampling site. In this

case, it is assumed a λ -dependence of b_{abs} related to the source of the absorbing aerosol as follows:

$$\frac{b_{abs,FF}(\lambda)}{b_{abs,FF}(\lambda_{ref})} = \left(\frac{\lambda}{\lambda_{ref}}\right)^{-\alpha_{FF}} \quad \frac{b_{abs,WB}(\lambda)}{b_{abs,WB}(\lambda_{ref})} = \left(\frac{\lambda}{\lambda_{ref}}\right)^{-\alpha_{WB}} \quad (4)$$

where α_{FF} and α_{WB} are the AAE representative for FF and WB aerosol and λ_{ref} can be arbitrarily chosen.

Moreover, the MWAA approach is based on the following assumptions:

- Wood burning is the only source of BrC;
- BC_{FF} and BC_{WB} have the same AAE (α_{BC}), disregarding the emission source;
- BC and BrC have different spectral dependences, i.e. different AAE (α_{BC} and α_{BrC} , respectively);

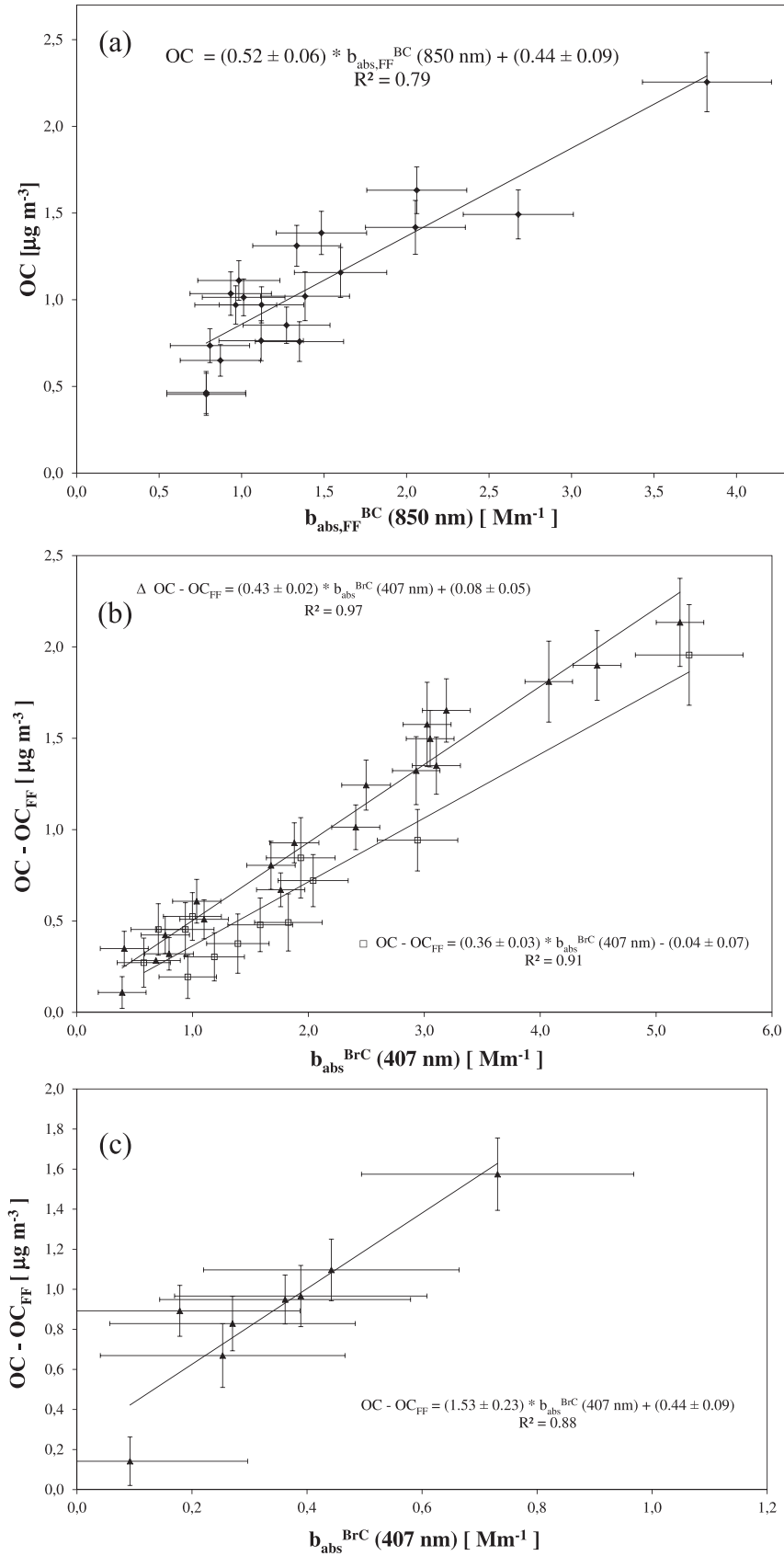


Fig. 4. Rural site dataset: (a) OC versus $b_{abs,FF}^{BrC}(850 \text{ nm})$ only for samples with $\alpha_{exp} \approx 1$; (b) $OC - OC_{FF}$ vs. $b_{abs}^{BrC}(407 \text{ nm})$ open squares refer to wintertime 2013 and full triangles to wintertime 2014; (c) $OC - OC_{FF}$ vs. $b_{abs}^{BrC}(407 \text{ nm})$ for samples collected in the warm period.

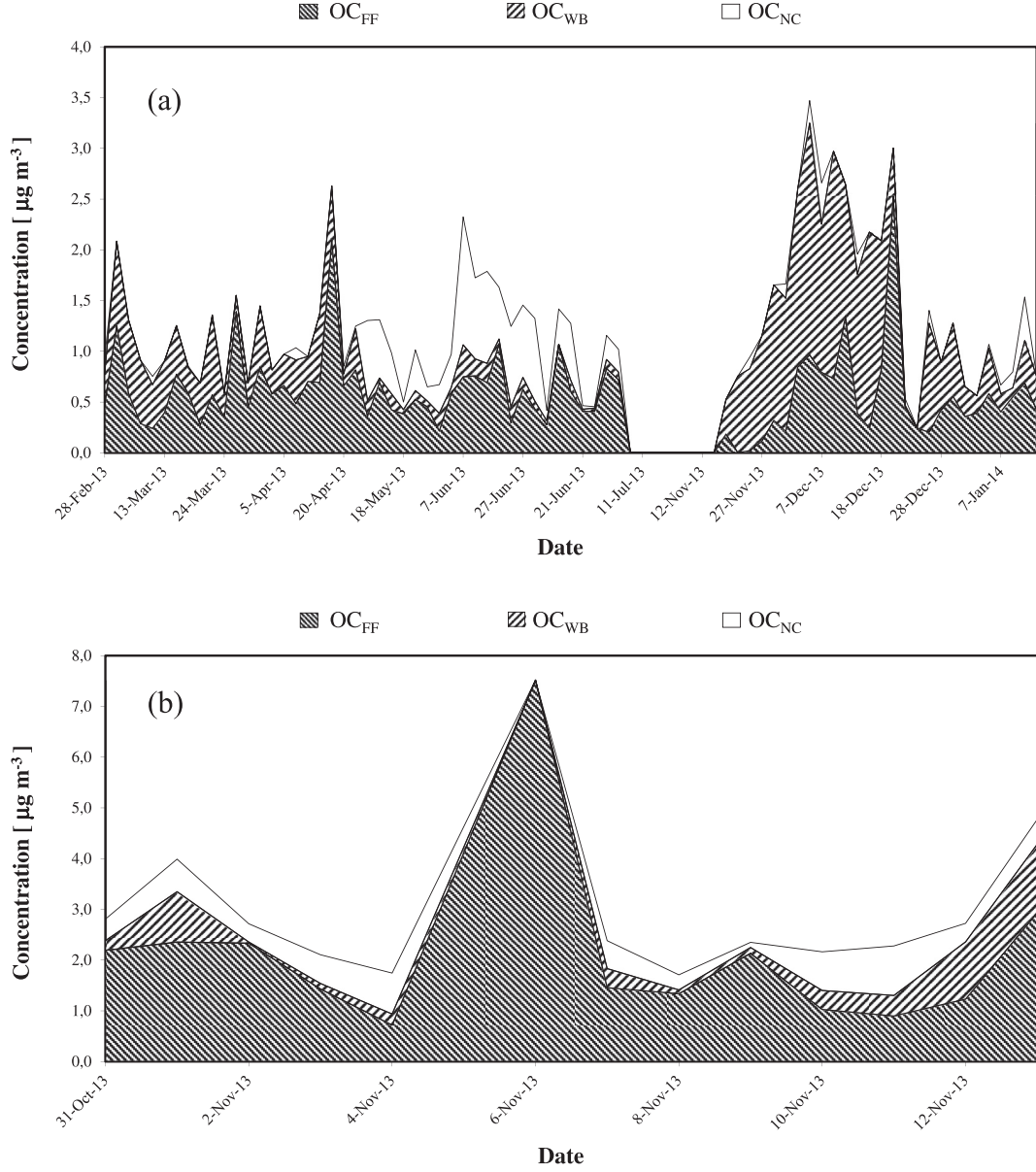


Fig. 5. OC apportionment for the rural site (a) and the urban background site (b).

d) Fossil fuels are assumed not to contribute to BrC, thus AAE for FF aerosol is assumed to be the one for BC ($\alpha_{\text{FF}} = \alpha_{\text{BC}}$). α_{FF} value was set as explained in the following;

e) α_{WB} was set to a fixed value as explained in the following.

Equations (1) and (2) can be joined and rewritten as:

$$\begin{aligned}
 b_{\text{abs}}(\lambda) &= \left[(BC_{\text{FF}} + BC_{\text{WB}}) \cdot \text{MAC}_{\lambda_{\text{ref1}}}^{\text{BC}} \right] \left(\frac{\lambda}{\lambda_{\text{ref1}}} \right)^{-\alpha_{\text{BC}}} + \left[\text{BrC} \cdot \text{MAC}_{\lambda_{\text{ref2}}}^{\text{BrC}} \right] \left(\frac{\lambda}{\lambda_{\text{ref2}}} \right)^{-\alpha_{\text{BrC}}} \\
 &= \underbrace{\left[(BC_{\text{FF}} + BC_{\text{WB}}) \cdot \frac{\text{MAC}_{\lambda_{\text{ref1}}}^{\text{BC}}}{\lambda_{\text{ref1}}^{-\alpha_{\text{BC}}}} \right]}_{\text{A}} \lambda^{-\alpha_{\text{BC}}} + \underbrace{\left[\text{BrC} \cdot \frac{\text{MAC}_{\lambda_{\text{ref2}}}^{\text{BrC}}}{\lambda_{\text{ref2}}^{-\alpha_{\text{BrC}}}} \right]}_{\text{B}} \lambda^{-\alpha_{\text{BrC}}} \\
 &= \underbrace{\left[(BC_{\text{FF}} + BC_{\text{WB}}) \cdot \sigma_0^{\text{BC}} \right]}_{\text{A}} \lambda^{-\alpha_{\text{BC}}} + \underbrace{\left[\text{BrC} \cdot \sigma_0^{\text{BrC}} \right]}_{\text{B}} \lambda^{-\alpha_{\text{BrC}}}
 \end{aligned} \tag{5}$$

Table 1

Average EC and OC apportionment at the two sites. Values are given as percentages of total measured EC and OC.

Site	<EC _{FF} >	<EC _{WB} >	<OC _{FF} >	<OC _{WB} >	<OC _{NC} >
Propata, winter 2013	68 ± 15	32 ± 11	63 ± 7	35 ± 10	7 ± 12
Propata, summer 2013	87 ± 19	13 ± 8	53 ± 4	11 ± 6	36 ± 12
Propata, winter 2014	47 ± 9	53 ± 9	38 ± 5	61 ± 5	4 ± 11
Genoa, fall 2013	84 ± 11	16 ± 7	67 ± 5	15 ± 5	19 ± 9

Where:

- $MAC_{\lambda_{ref1}}^{BC}$ and $MAC_{\lambda_{ref2}}^{BrC}$ are the mass specific absorption coefficients (in $[m^2 g^{-1}]$) at arbitrarily chosen reference wavelengths (λ_{ref1} and λ_{ref2}) for BC and BrC, respectively; it is noteworthy that $\sigma_0^{BC} = MAC_{\lambda_{ref1}}^{BC} / \lambda_{ref1}^{-\alpha_{BC}}$ and $\sigma_0^{BrC} = MAC_{\lambda_{ref2}}^{BrC} / \lambda_{ref2}^{-\alpha_{BrC}}$ only depend on BC and BrC properties, respectively.
- BC_{FF} and BC_{WB} are the concentrations of BC emitted by FF and WB, respectively;
- BrC is the concentration of brown carbon. The indication of the BrC source is omitted as we assume it comes only from WB.

With the same formalism introduced for Eq. (5), Eqs. (3) and (4) are joined and rewritten as:

$$b_{abs}(\lambda) = \underbrace{[BC_{FF} \cdot \sigma_0^{BC}]}_A \lambda^{-\alpha_{FF}} + \underbrace{[BC_{WB} \cdot \sigma_0^{BC} + BrC \cdot \sigma_0^{BrC}]}_B \lambda^{-\alpha_{WB}} \quad (6)$$

Many works (Bond and Bergstrom, 2006; Moosmüller et al., 2011; and references therein) show that aerosol produced by fossil fuel combustion has a typical value of $\alpha_{FF} \approx 1.0$, considering laboratory as well as field experiments, thus meaning an inverse proportionality between b_{abs} and λ . This further supports our assumption that $\alpha_{FF} = \alpha_{BC}$, that means that OC_{FF} is expected not to contribute to $b_{abs,FF}$ (i.e. no BrC is emitted by FF combustion). Indeed, in samples where negligible WB contribution is expected because of low levoglucosan concentration, a $\lambda^{-\alpha_{exp}}$ function with $0.9 < \alpha_{exp} < 1.1$ suitably fits the $5-\lambda$ determined b_{abs} . Considering α_{BC} , it is widely accepted that the absorption cross-section for “pure” BC in the atmosphere varies as λ^{-1} , i.e. the imaginary part of the refractive index does not depend on λ (Bond and Bergstrom, 2006; Lack and Langridge, 2013; and references therein). Taking

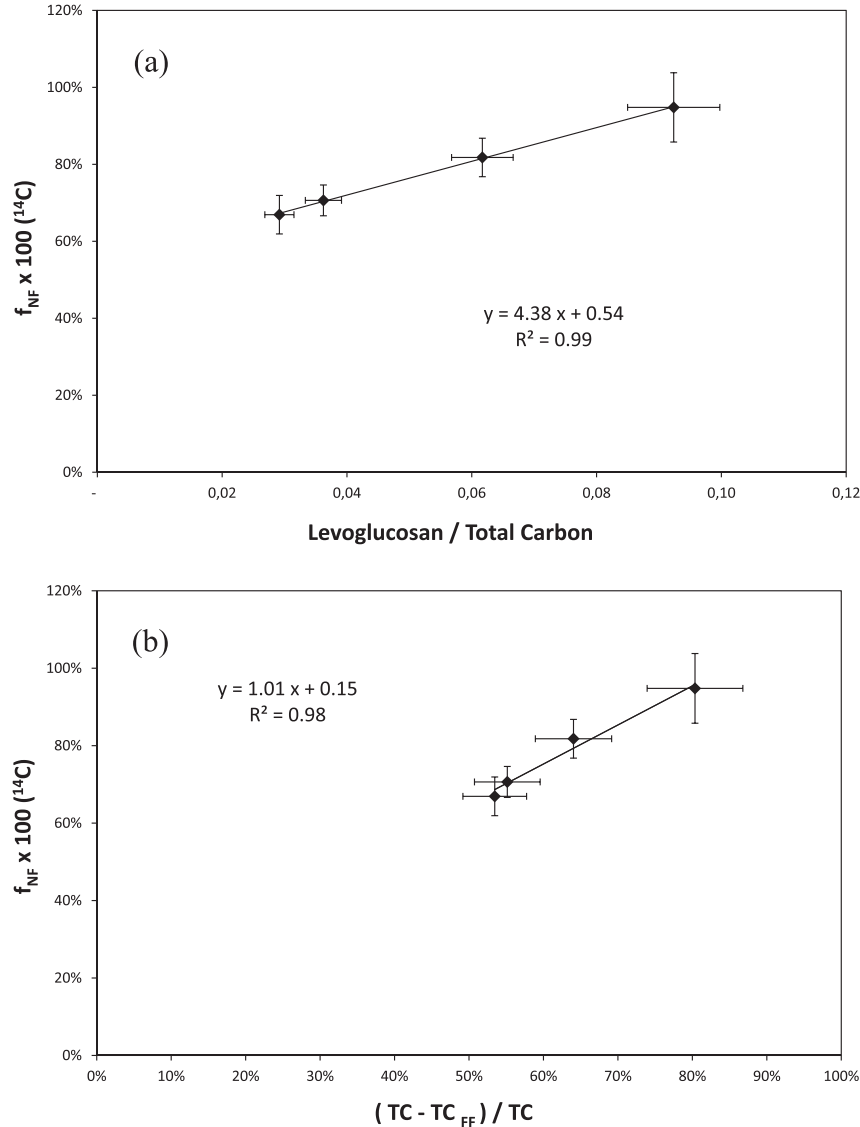


Fig. 6. Rural site high volume samples: (a) f_{NF} vs. levoglucosan/TC; (b) f_{NF} vs. $TC - TC_{FF}$ obtained by the optical approach ($TC_{FF} = EC_{FF} + OC_{FF}$).

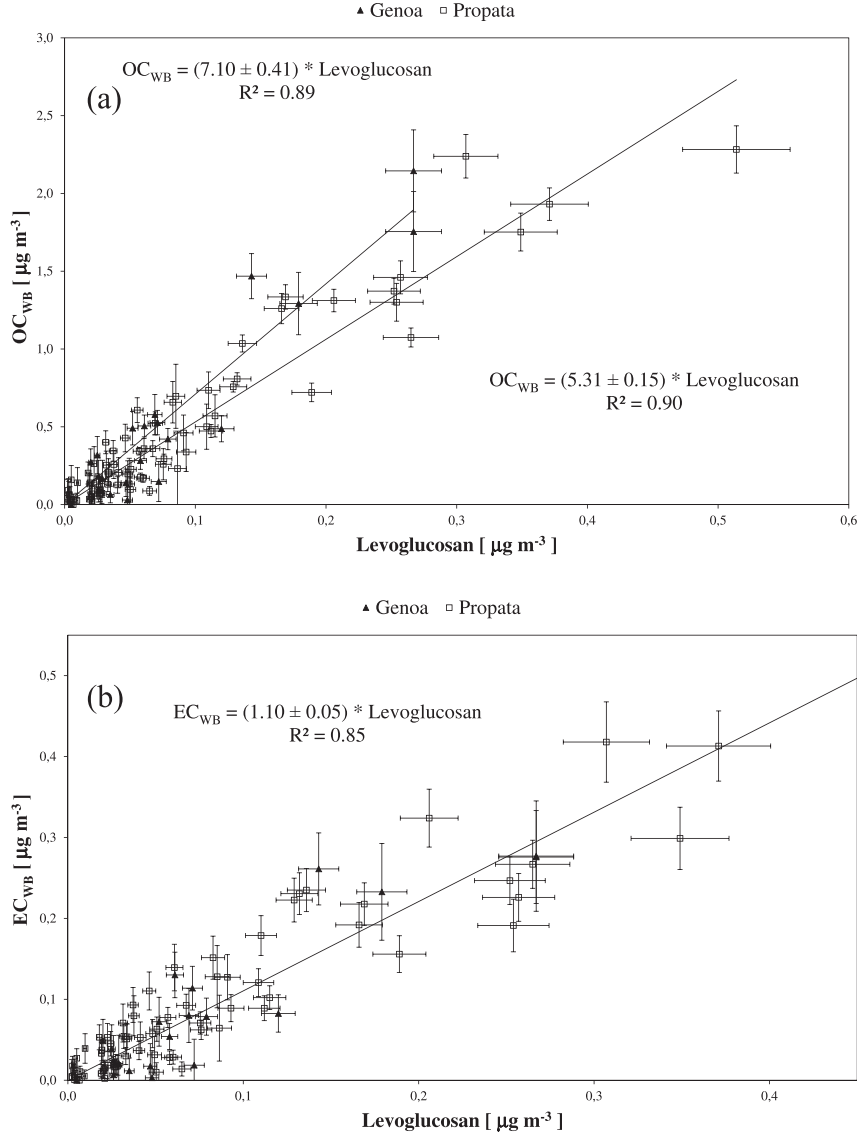


Fig. 7. (a) OC_{WB} vs. levoglucosan and (b) EC_{WB} vs. levoglucosan. In the case of OC_{WB} two different OC_{WB} to levoglucosan ratios were found for Propata (open squares) and Genoa (full triangles).

into account the previous considerations, in this study we fixed $\alpha_{\text{FF}} = 1.0$ (see further discussion at §4).

In the case of woodsmoke, α_{WB} values are generally in the range of 0.9–2.2 (Harrison et al., 2013; and therein cited literature) depending on several factors as air mass aging and the type of wood burnt as well as the specific wavelength range where the α_{WB} values are calculated. In this work, we fixed $\alpha_{\text{WB}} = 1.8$ which gave a fairly good agreement with independent ^{14}C measurements (see discussion at §4). Once α_{BC} , α_{FF} and α_{WB} have been set, the system is numerically solved by fitting the two Eqs. (5) and (6) separately and using a MINUIT χ^2 minimization routine (James, 1978) home-written as a C++ program (ROOT package; Brun and Rademakers, 1997). The minimization program fits the 5- λ b_{abs} measurements performed by MWAA following Eqs. (5) and (6) to obtain A, B, A', B' and α_{BrC} for each sample. It is noteworthy the multi- λ measurements allow to run the proposed model and provide an accurate fitting. The mean α_{BrC} values extracted for the Propata and Genoa datasets are 3.89 ± 0.18 and 4.02 ± 0.19 , respectively (quoted uncertainties are the standard deviation of the two distributions). Values of α_{BrC} up to 9.5 have been reported for wavelength pairs

400 and 700 nm (Lack and Langridge, 2013; and references therein). The values obtained in this work are in good agreement with the findings of Yang et al. (2009) who reported $\alpha_{\text{BrC}} = 3.5$ (for wavelength pairs 470 and 660 nm).

Considering Eqs. (5) and (6), the following relations can be derived:

$$\begin{cases} A - A' = \text{BC}_{\text{WB}} \sigma_0^{\text{BC}} \\ A' = \text{BC}_{\text{FF}} \sigma_0^{\text{BC}} \\ B = \text{BrC} \sigma_0^{\text{BC}} \end{cases}$$

and the corresponding λ dependences lead to:

$$\begin{cases} b_{\text{abs}, \text{WB}}^{\text{BC}}(\lambda) = \text{BC}_{\text{WB}} \sigma_0^{\text{BC}} \lambda^{-\alpha_{\text{BC}}} = (A - A') \lambda^{-\alpha_{\text{BC}}} \\ b_{\text{abs}, \text{FF}}^{\text{BC}}(\lambda) = \text{BC}_{\text{FF}} \sigma_0^{\text{BC}} \lambda^{-\alpha_{\text{BC}}} = A' \lambda^{-\alpha_{\text{BC}}} \\ b_{\text{abs}}^{\text{BrC}}(\lambda) = \text{BrC} \sigma_0^{\text{BrC}} \lambda^{-\alpha_{\text{BrC}}} = B \lambda^{-\alpha_{\text{BrC}}} \end{cases} \quad (7)$$

thus the source-dependent (FF or WB) light absorption contributions to BC and BrC ($b_{\text{abs}, \text{FF}}^{\text{BC}}(\lambda)$, $b_{\text{abs}, \text{WB}}^{\text{BC}}(\lambda)$, and $b_{\text{abs}}^{\text{BrC}}(\lambda)$) can be

obtained from the results of the minimization algorithm. Please note that BrC is assumed to be emitted only by WB, thus the source indication is omitted in b_{abs}^{BrC} .

In Fig. 1, the mean $b_{abs}(\lambda)$ source apportionment at the rural site of Propata is shown. Moreover, the optical apportionment for the Propata winter campaign is shown as an example in Fig. 2 at $\lambda = 850$ nm and $\lambda = 375$ nm. As expected, the Figures show that b_{abs}^{BrC} is very low at the infrared (IR) wavelength whereas it explains up to 50% of the total light absorption in the case of UV. Although $b_{abs}^{BrC}(850$ nm) is generally low, it varies greatly from one day to another reaching values up to 11% of the total $b_{abs}(850$ nm).

4.2. Mass apportionment: equivalent black carbon (EBC)

The MWA approach described so far quantifies the three main contributors to total b_{abs} ($b_{abs,FF}^{BC}$, $b_{abs,WB}^{BC}$, and b_{abs}^{BrC}) at five different λ , so that:

$$b_{abs}(\lambda) = b_{abs,FF}^{BC}(\lambda) + b_{abs,WB}^{BC}(\lambda) + b_{abs}^{BrC}(\lambda) \quad (8)$$

Moreover, following the approach in Eq. (5) a wavelength-dependent mass-absorption cross-section for BC can be introduced as $MAC^{BC}(\lambda) = \sigma_0^{BC} \lambda^{-\alpha_{BC}} = \sigma_0^{BC} \lambda^{-1}$. This allows the evaluation of the equivalent black carbon in atmosphere (EBC) as the sum of EBC from FF and WB (EBC_{FF} and EBC_{WB} , respectively):

$$EBC = EBC_{FF} + EBC_{WB} = \frac{b_{abs,FF}^{BC}(\lambda) + b_{abs,WB}^{BC}(\lambda)}{MAC^{BC}(\lambda)} \quad (9)$$

With the further assumption of equivalence between the EBC in atmosphere and the EC determined by thermal-optical analysis ($EBC_{FF} = EC_{FF}$ and $EBC_{WB} = EC_{WB}$), the following relationships hold at every λ :

$$\begin{aligned} EC_{FF} &= EC - EC_{WB} = EC \left(1 - \frac{EC_{WB}}{EC} \right) = EC \left(1 - \frac{b_{abs,WB}^{BC}}{b_{abs}^{BC}} \right) \\ &= EC \left(1 - \frac{b_{abs,WB}^{BC}}{b_{abs} - b_{abs}^{BrC}} \right) = EC \left(\frac{b_{abs} - b_{abs}^{BrC} - b_{abs,WB}^{BC}}{b_{abs} - b_{abs}^{BrC}} \right) \end{aligned} \quad (10)$$

Focusing on the IR range where BrC contribution to total b_{abs} is minimized (thus reducing uncertainties on the denominator evaluation) we obtain:

$$EC_{FF} = EC \frac{b_{abs,FF}^{BC}(850 \text{ nm})}{b_{abs}(850 \text{ nm}) - b_{abs}^{BrC}(850 \text{ nm})} \quad (11)$$

$$EC_{WB} = EC \frac{b_{abs,WB}^{BC}(850 \text{ nm})}{b_{abs}(850 \text{ nm}) - b_{abs}^{BrC}(850 \text{ nm})} \quad (12)$$

Fig. 3 shows the EC apportionment deduced by Eqs. (11) and (12) at Propata and Genoa. EC_{WB} is higher in winter while it becomes small or almost zero during summertime. The resulting $MAC^{BC}(850$ nm) is $(6.57 \pm 0.13) \text{ m}^2 \text{ g}^{-1}$ ($R^2 = 0.87$) and $(6.40 \pm 0.10) \text{ m}^2 \text{ g}^{-1}$ ($R^2 = 0.98$) for Propata and Genoa, respectively. As the two values are comparable within the experimental uncertainties, the mean value is calculated $< MAC^{BC}(850 \text{ nm}) \geq 6.5 \pm 0.10 \text{ m}^2 \text{ g}^{-1}$. However, it is worthy to note that generally the MAC^{BC} is an apparent, site-specific value including ambient factors as reported in several works (Bond and Bergstrom, 2006).

4.3. Mass apportionment: organic carbon

The OC source apportionment is less straightforward as not

light-absorbing carbon as well as non-combustion components (OC_{NC}) such as spores, pollen, etc. can contribute to OC. The OC values determined by the TOT analysis can be thus expressed as:

$$OC = OC_{FF} + OC_{WB} + OC_{NC} \quad (13)$$

In the following, all the biogenic compounds are considered as not optically active and they are summed up in the OC_{NC} term. Moreover, BrC is assumed to be produced only by the WB source; this is actually confirmed by the inter-comparison discussed in §4 (see also Zheng et al., 2013).

To perform the OC apportionment, it is assumed a linear relationship between BC_{FF} and OC_{FF} as well as between BrC and OC_{WB} (i.e. BC_{FF} and BrC are used as tracers for FF and WB sources, respectively). Moreover, the linear relationship between BC_{FF} and BrC and their absorption coefficients allows re-writing Eq. (13) as:

$$OC = k_1 \cdot \underbrace{b_{abs,FF}^{BC}(850 \text{ nm})}_{OC_{FF}} + k_2 \cdot \underbrace{b_{abs}^{BrC}(407 \text{ nm})}_{OC_{WB}} + OC_{NC} \quad (14)$$

where:

- OC is the organic carbon concentration in [$\mu\text{g m}^{-3}$] measured by TOT analysis;
- $b_{abs,FF}^{BC}(850 \text{ nm})$ in [Mm^{-1}] is the contribution to the BC_{FF} absorption @ $\lambda = 850$ nm;
- $b_{abs}^{BrC}(407 \text{ nm})$ in [Mm^{-1}] is the contribution to the BrC absorption @ $\lambda = 407$ nm;
- k_1 is a constant coefficient in [g m^{-2}] related to the $MAC^{BC}(850 \text{ nm})$ and to OC_{FF}/BC_{FF} ;
- k_2 is a constant coefficient in [g m^{-2}] related to the BrC MAC @ $\lambda = 407$ nm and to OC_{WB}/BrC ;
- OC_{NC} is expressed in [$\mu\text{g m}^{-3}$].

The absorption coefficient determined at $\lambda = 850$ nm and 407 nm where chosen as starting points for OC_{FF} and OC_{WB} determination. The choice of $\lambda = 407$ nm as reference for the evaluation of BrC contribution is related to the unavailability of the laser diode with $\lambda = 375$ nm during the first winter campaign.

With our approach, both k_1 and k_2 are directly determined by the experimental optical data. In samples where the α_{exp} is close to 1.0 (i.e. the measured $b_{abs}(\lambda)$ approximately follows λ^{-1}) b_{abs}^{BrC} is negligible, thus Eq. (14) reduces to:

$$OC \approx k_1 \cdot b_{abs,FF}^{BC}(850 \text{ nm}) + OC_{NC} \quad \text{when} \quad \alpha_{exp} \approx 1 \quad (15)$$

The k_1 parameter is then determined by a regression study of OC vs. $b_{abs,FF}^{BC}$ restricted to the samples with $\alpha_{exp} \approx 1$.

Such analysis on the rural site dataset is shown in Fig. 4a and gives $k_1 = 0.52 \pm 0.06$ ($R^2 = 0.79$). Once determined k_1 – and thus the OC_{FF} contribution for each sample – k_2 can be calculated by performing another linear regression involving the remaining part of the dataset:

$$OC - OC_{FF} = k_2 \cdot b_{abs}^{BrC}(407 \text{ nm}) + OC_{NC} \quad (16)$$

Whereas k_1 remains nearly constant during the whole campaign (data in Fig. 4a span all over the year), the value of k_2 is season-dependent: in the cold period of 2013 (approximately February–March 2013), the regression study (Fig. 4b, open squares) gives $k_2 = 0.36 \pm 0.03$ ($R^2 = 0.91$) while in the warm period (approximately between May and July 2013, Fig. 4c) k_2 is 1.53 ± 0.23 ($R^2 = 0.88$). In the last part of the campaign (between November 2013 and February 2014) k_2 is again very close to the value found in the cold period of 2013 (Fig. 4b, full triangles) with a value of

0.43 ± 0.02 ($R^2 = 0.97$). In this analysis, transition days between cold and warm periods are not taken into account. Once determined k_1 and k_2 , OC_{FF} and OC_{WB} are calculated for each sample and OC_{NC} is obtained by Eq. (13). In Propata, OC_{WB} concentration values are typically high during wintertime and especially during late fall 2013 (Fig. 5a). The OC_{FF} fraction is similar all over the year with a percentage increase in early springtime. OC_{NC} concentration values are mostly negligible during the cold periods while they increase to a mean $\langle OC_{NC} \rangle = (0.44 \pm 0.10) \mu\text{g m}^{-3}$ during late spring and summer. In Genoa, the OC_{FF} fraction is dominant during the whole campaign accounting for about 70% of total OC (Fig. 5b). In Table 1 a summary of the apportionment results for the two sites is reported.

5. Comparison with independent techniques

The reliability of the optical mass apportionment was checked by independent levoglucosan and ^{14}C measurements. The comparison between parallel determinations (please note that radiocarbon measurements have been performed on 4 samples only, see §2) is shown in Fig. 6a.

A very good agreement between f_{NF} by radiocarbon measurements and levoglucosan/TC is found (slope = 4.38, $R^2 = 0.99$). The intercept value (55%) can be probably attributed to local background secondary organic aerosol, as the possible biogenic contribution seems to be negligible according to the optical apportionment (Fig. 5a).

The best agreement between the results obtained by our optical approach and radiocarbon measurements is found for $\alpha_{WB} = 1.8$ (Fig. 6b); this value is similar to $\alpha_{WB} = 1.86$ found by Sandradewi et al. (2008).

Literature works (Favez et al., 2010; Sandradewi et al., 2008; Harrison et al., 2013) showed the sensitivity of the Aethalometer model results to the a priori setting of α_{FF} and α_{WB} . In this work, few trials changing the values assumed for α_{BC} , α_{FF} , and α_{WB} were carried out; among them, the one most affecting the regression parameters in Fig. 6b is α_{WB} . Indeed, varying this parameter by ± 0.1 a change in the slope of about $\pm 10\%$ and in the intercept by $\pm 8\%$ is observed.

Furthermore, for the low volume samples the reliability of the optical mass apportionment was verified versus the independent determination of the levoglucosan concentration. In Fig. 7a the following results are reported: $OC_{WB} = (5.31 \pm 0.15) \cdot \text{levoglucosan}$ ($R^2 = 0.90$) at the rural background site in Propata and $OC_{WB} = (7.10 \pm 0.41) \cdot \text{levoglucosan}$ ($R^2 = 0.89$) at the urban background site in Genoa. Especially in Propata, the determined OC_{WB} to levoglucosan concentration ratio is in very good agreement with results by Piazzalunga et al. (2011), Bernardoni et al. (2011), and Favez et al. (2010) who used $OM_{WB}/\text{levoglucosan} \sim 10.8$ and $OM_{WB}/OC_{WB} = 1.8$. A good correlation with levoglucosan was found for EC_{WB} too; the regression study (Fig. 7b) gave $EC_{WB} = (1.10 \pm 0.05) \cdot \text{levoglucosan}$ ($R^2 = 0.85$) with no significant differences between the two datasets. On the contrary, the levoglucosan concentration values do not show any correlation with the EC_{FF} and OC_{FF} values.

We can therefore conclude that, at the present level of knowledge, $\alpha_{WB} = 1.8 \pm 0.1$ is a reliable figure for future uses of the optical apportionment methodology.

6. Conclusions

The MWAA can measure offline the aerosol absorption coefficient at 5 wavelengths ranging from IR to UV. In this way, a new apportionment methodology based on the so-called Aethalometer model but fully exploiting the multi-wavelength approach, can be applied to monitor the variability of WB and FF contributions to aerosol optical absorption and mass concentration.

The model results depend on the choice of α_{BC} , α_{FF} , and α_{WB} values in Eqs. (4) and (5): in the present study, they have been fixed according to the recent literature and validated against independent techniques ($\alpha_{BC} = \alpha_{FF} = 1.0$; $\alpha_{WB} = 1.8$). Although these values in principle can be site-dependent and modified in future works, the data reduction approach here proposed remains valid. The optical apportionment is based on the assumption that the absorbing species in aerosols are related to FF and WB only. In case of significant dust intrusions, this might be not true and could lead to inaccurate source apportionment. The possible optical activity of biogenic compounds is also neglected in this work but this issue merits a further investigation. Despite of the mentioned limitations, in this paper we introduce a new methodology which produces sounding results both at a rural site and in a large coastal city in Italy.

Acknowledgements

This work was partially financed by the National Institute of Nuclear Physics (INFN) in the frame of the MANIA experiment and by the Amministrazione Provinciale di Genova. The authors acknowledge Vincenzo Ariola, Franco Parodi, and Francesco Saffioti (INFN-Genova) for technical support in the MWAA development and Maria Teresa Zannetti and Federico Manni (Amministrazione Provinciale di Genova) for the collaboration during sampling.

References

- Ajtai, T., Filep, Á., Schnaiter, M., Linke, C., Vragel, M., Bozókí, Z., Szabó, G., Leisner, T., 2010. A novel multi-wavelength photoacoustic spectrometer for the measurement of the UV-vis-NIR spectral absorption coefficient of atmospheric aerosols. *J. Aerosol Sci.* 41, 1020–1029.
- Andreae, M.O., 2001. The dark side of aerosols. *Nature* 409, 671–672.
- Andreae, M.O., Gelencsér, A., 2006. Black carbon or brown carbon? The nature of light-absorbing carbonaceous aerosol. *Atmos. Chem. Phys.* 6, 3131–3148.
- Bernardoni, V., Vecchi, R., Valli, G., Piazzalunga, A., Fermo, P., 2011. PM10 source apportionment in Milan (Italy) using time-resolved data. *Sci. Total Environ.* 409, 4788–4795.
- Bernardoni, V., Calzolari, G., Chiari, M., Fedi, M., Lucarelli, F., Nava, S., Piazzalunga, A., Riccobono, F., Taccetti, F., Valli, G., Vecchi, R., 2013. Radiocarbon analysis on organic and elemental carbon in aerosol samples and source apportionment at an urban site in Northern Italy. *J. Aerosol Sci.* 56, 88–99.
- Bond, T.C., Anderson, T.L., Campbell, D., 1999. Calibration and intercomparison of filter-based measurements of visible light absorption by aerosols. *Aerosol Sci. Technol.* 30, 582–600.
- Bond, T.C., Bergstrom, R.W., 2006. Light absorption by carbonaceous particles: an investigative review. *Aerosol Sci. Technol.* 40, 27–67.
- Bond, T.C., Doherty, S.J., Fahey, D.W., Forster, P.M., Berntsen, T., DeAngelo, B.J., Flanner, M.G., Ghan, S., Kärcher, B., Koch, D., Kinne, S., Kondo, Y., Quinn, P.K., Sarofim, M.C., Schultz, M.G., Schulz, M., Venkataraman, C., Zhang, H., Zhang, S., Bellouin, N., Guttikunda, S.K., Hopke, P.K., Jacobson, M.Z., Kaiser, J.W., Klimont, Z., Lohmann, U., Schwarz, J.P., Shindell, D., Storelvmo, T., Warren, S.G., Zender, C.S., 2013. Bounding the role of black carbon in the climate system: a scientific assessment. *J. Geophys. Res. Atmos.* 118, 5380–5552.
- Brun, R., Rademakers, F., 1997. ROOT-an object oriented data analysis framework. *Nucl. Instrum. Methods Phys. Res. Sect. A Accel. Spectrom. Detect. Assoc. Equip.* 389, 81–86.
- Calzolari, G., Bernardoni, V., Chiari, M., Fedi, M., Lucarelli, F., Nava, S., Riccobono, F., Taccetti, F., Valli, G., Vecchi, R., 2011. The new sample preparation line for radiocarbon measurements on atmospheric aerosol at LABEC. *Nucl. Instrum. Methods Phys. Res. Sect. B Beam Interact. Mater. Atoms* 269, 203–208.
- Cavalli, F., Putaud, J.P., Viana, M., Yttri, K.E., Gemberg, J., 2010. Toward a standardized thermal-optical protocol for measuring atmospheric organic and elemental carbon: the EUSAAR protocol. *Atmos. Meas. Tech.* 3, 79–89.
- Collaud Coen, M., Weingartner, E., Apituley, A., Ceburnis, D., Fierz-Schmidhauser, R., Flentje, H., Henzing, J.S., Jennings, S.G., Moerman, M., Petzold, A., Schmid, O., Baltensperger, U., 2010. Minimizing light absorption measurement artifacts of the Aethalometer: evaluation of five correction algorithms. *Atmos. Meas. Tech.* 3, 457–474.
- Favez, O., El Haddad, I., Piot, C., Boreave, A., Abidi, E., Marchand, N., Jaffrezo, J.L., Besombes, J.L., Personnaz, M.B., Sciare, J., Wortham, H., Geroge, C., D'Anna, B., 2010. Inter-comparison of source apportionment models for the estimation of wood burning aerosols during wintertime in an Alpine city (Grenoble, France). *Atmos. Chem. Phys.* 10, 5295–5314.
- Fedi, M.E., Bernardoni, V., Caforio, L., Calzolari, G., Carraresi, L., Manetti, M., Taccetti, F., Mando, P.A., 2013. Status of sample combustion and graphitization

- lines at INFN-LABEC, Florence. *Radiocarbon* 55, 657–664.
- Filep, Á., Ajtai, T., Utry, N., Pintér, M.D., Nyilas, T., Takács, S., Máté, Z., Gelencsér, A., Hoffer, A., Schnaiter, M., Bozóki, Z., Szabó, G., 2013. Absorption spectrum of ambient aerosol and its correlation with size distribution in specific atmospheric conditions after a Red Mud Accident. *Aerosol Air Qual. Res.* 13, 49–59.
- Flowers, B.A., Dubey, M.K., Mazzoleni, C., Stone, E.A., Schauer, J.J., Kim, S.-W., Yoon, S.C., 2010. Optical-chemical-microphysical relationships and closure studies for mixed carbonaceous aerosols observed at Jeju Island; 3-laser photoacoustic spectrometer, particle sizing, and filter analysis. *Atmos. Chem. Phys.* 10, 10387–10398.
- Hänel, G., 1987. Radiation budget of the boundary layer: Part II. Simultaneous measurement of mean solar volume absorption and extinction coefficients of particles. *Beitr. Phys. Atmos.* 60, 241–247.
- Hänel, G., 1994. Optical properties of atmospheric particles: complete parameter sets obtained through polar photometry and an improved inversion technique. *Appl. Opt.* 33, 7187–7199.
- Harrison, R.M., Beddows, D.C.S., Jones, A.M., Calvo, A., Alves, C., Pio, C., 2013. An evaluation of some issues regarding the use of aethalometers to measure woodsmoke concentrations. *Atmos. Environ.* 80, 540–548.
- James, F., 1978. MINUIT, a Package of Programs to Minimise a Function of N Variables, Compute the Covariance Matrix, and Find the True Errors. Program library code D507. CERN.
- Kirchstetter, T.W., Novakok, T., Hobbs, P.V., 2004. Evidence that the spectral dependence of light absorption by aerosols is affected by organic carbon. *J. Geophys. Res.* 109, D21208.
- Kirchstetter, T.W., Thatcher, T.L., 2012. Contribution of organic carbon to wood smoke particulate matter absorption of solar radiation. *Atmos. Chem. Phys.* 12, 6067–6072.
- Lack, D.A., Langridge, J.M., 2013. On the attribution of black and brown carbon light absorption using the Ångström exponent. *Atmos. Chem. Phys.* 13, 10535–10543.
- Lewis, K., Arnott, W.P., Moosmüller, H., Wold, C.E., 2008. Strong spectral variation of biomass smoke light absorption and single scattering albedo observed with a novel dual-wavelength photoacoustic instrument. *J. Geophys. Res.* 113, D16203.
- Linke, C., Möhler, O., Veres, A., Mohácsi, Á., Bozóki, Z., Szabó, G., Schnaiter, M., 2006. Optical properties and mineralogical composition of different Saharan mineral dust samples: a laboratory study. *Atmos. Chem. Phys.* 6, 3315–3323.
- Massabò, D., Bernardoni, V., Bove, M.C., Brunengo, A., Cuccia, E., Piazzalunga, A., Prati, P., Valli, G., Vecchi, R., 2013. A multi-wavelength optical set-up for the characterization of carbonaceous particulate matter. *J. Aerosol Sci.* 60, 34–46.
- Moosmüller, H., Chakrabarty, R.K., Arnott, W.P., 2009. Aerosol light absorption and its measurement: a review. *J. Quant. Spectrosc. Radiat. Transf.* 110, 844–878.
- Moosmüller, H., Chakrabarty, R.K., Ehlers, K.M., Arnott, W.P., 2011. Absorption Ångström coefficient, brown carbon, and aerosols: basic concepts, bulk matter, and spherical particles. *Atmos. Chem. Phys.* 11, 1217–1225.
- Müller, T., Henzing, J.S., de Leeuw, G., Wiedensohler, A., Alastuey, A., Angelov, H., Bizjak, M., Collaud Coen, M., Engström, J.E., Gruening, C., Hillamo, R., Hoffer, A., Imre, K., Ivanov, P., Jennings, G., Sun, J.Y., Kalivitis, N., Karlsson, H., Komppula, M., Laj, P., Li, S.-M., Lunder, C., Marinoni, A., Martins dos Santos, S., Moerman, M., Nowak, A., Ogren, J.A., Petzold, A., Pichon, J.M., Rodriguez, S., Sharma, S., Sheridan, P.J., Teinilä, K., Tuch, T., Viana, M., Virkkula, A., Weingartner, E., Wilhelm, R., Wang, Y.Q., 2011. Characterization and intercomparison of aerosol absorption photometers: result of two intercomparison workshops. *Atmos. Meas. Tech.* 4, 245–268.
- Petzold, A., Schöllner, M., 2004. Multi-angle absorption photometry – a new method for the measurement of aerosol light absorption and atmospheric black carbon. *J. Aerosol Sci.* 35, 421–441.
- Petzold, A., Schloesser, H., Sheridan, P.J., Arnott, W.P., Ogren, J.A., Virkkula, A., 2005. Evaluation of multiangle absorption photometry for measuring aerosol light absorption. *Aerosol Sci. Technol.* 39 (1).
- Piazzalunga, A., Fermo, P., Bernardoni, V., Vecchi, R., Valli, G., De Gregorio, M.A., 2010. A simplified method for levoglucosan quantification in wintertime atmospheric particulate matter by high performance anion-exchange chromatography coupled with pulsed amperometric detection. *Int. J. Environ. Anal. Chem.* 90, 934–947.
- Piazzalunga, A., Belis, C., Bernardoni, V., Cazzuli, O., Fermo, P., Valli, G., Vecchi, R., 2011. Estimates of wood burning contribution to PM by the macro-tracer method using tailored emission factors. *Atmos. Environ.* 45, 6642–6649.
- Pöschl, U., 2003. Aerosol particle analysis: challenges and progress. *Anal. Bioanal. Chem.* 375, 3032.
- Sandradewi, J., Prevot, A.H., Szidat, S., Perron, N., Rami Alfarra, M., Lanz, V., Weingartner, E., Baltensperger, U., 2008. Using aerosol light absorption measurements for the quantitative determination of Wood burning and traffic emission contributions to particulate matter. *Environ. Sci. Technol.* 42, 3316–3323.
- Simoneit, B.R.T., Schauer, J.J., Nolte, C.G., Oros, D.R., Elias, V.O., Fraser, M.P., Rogge, W.F., Cass, G.R., 1999. Levoglucosan, a tracer for cellulose in biomass burning and atmospheric particles. *Atmos. Environ.* 33, 173–182.
- Utry, N., Ajtai, T., Filep, Á., Pintér, M.D., Hoffer, A., Bozóki, Z., Szabó, G., 2013. Mass specific optical absorption coefficient of HULIS aerosol measured by a four-wavelength photoacoustic spectrometer at NIR, VIS and UV wavelengths. *Atmos. Environ.* 69, 321–324.
- Utry, N., Ajtai, T., Filep, Á., Pintér, M., Török, Zs., Bozóki, Z., Szabó, G., 2014. Correlations between absorption Ångström exponent (AAE) of wintertime ambient urban aerosol and its physical and chemical properties. *Atmos. Environ.* 91, 52–59.
- Vecchi, R., Bernardoni, V., Paganelli, C., Valli, G., 2014. A filter-based light-absorption measurement with polar photometer: effects of sampling artefacts from organic carbon. *J. Aerosol Sci.* 70, 15–25.
- Yang, M., Howell, S.G., Zhuang, J., Huebert, B.J., 2009. Attribution of aerosol light absorption to black carbon, brown carbon, and dust in China – interpretations of atmospheric measurements during EAST-AIRE. *Atmos. Chem. Phys.* 9, 2035–2050.
- Zheng, G., He, K., Duan, F., Cheng, Y., Ma, Y., 2013. Measurement of humic-like substances in aerosols: a review. *Environ. Pollut.* 181, 301–314.
- Zotter, P., El-Haddad, I., Zhang, Y., Hayes, P.L., Zhang, X., Lin, Y.-H., Wacker, L., Schnelle-Kreis, J., Abbaszade, G., Zimmermann, R., Surratt, J.D., Weber, R., Jimenez, J.L., Szidat, S., Baltensperger, U., Prévôt, A.S.H., 2014. Diurnal cycle of fossil and non fossil carbon using radiocarbon analyses during CalNex. *J. Geophys. Res. Atmos.* 119, 6818–6835.